

This is the final Version of Record of:

Citti, G., B. Franceschiello, G. Sanguinetti, e A. Sarti. «Sub-Riemannian Mean Curvature Flow for Image Processing». SIAM Journal on Imaging Sciences 9, n. 1 (1 gennaio 2016): 212–37.

The final published version is available online at:
<https://doi.org/10.1137/15M1013572>

Rights / License:

The terms and conditions for the reuse of this version of the manuscript are specified in the publishing policy. For all terms of use and more information see the publisher's website.

This item was downloaded from IRIS Università di Bologna (<https://cris.unibo.it/>)

When citing, please refer to the published version.

Sub-Riemannian Mean Curvature Flow for Image Processing*

G. Citti[†], B. Franceschiello[‡], G. Sanguinetti[§], and A. Sarti[‡]

Abstract. In this paper we reconsider the sub-Riemannian cortical model of image completion introduced in [G. Citti and A. Sarti, *J. Math. Imaging Vision*, 24 (2006), pp. 307–326]. This model combines two mechanisms, the sub-Riemannian diffusion and the concentration, giving rise to a diffusion driven motion by curvature. In this paper we give a formal proof of the existence of viscosity solutions of the sub-Riemannian motion by curvature. Furthermore we illustrate the sub-Riemannian finite difference scheme used to implement the model and we discuss some properties of the algorithm. Finally results of completion and enhancement on a number of natural images are shown and compared with other models.

Key words. image completion, sub-Riemannian models, existence result

AMS subject classifications. 68U10, 58J35, 35H20

DOI. 10.1137/15M1013572

1. Introduction. In this work we address the problem of completion (also known as inpainting) and contours enhancement: both require an analysis of elongated structures, such as level lines or contours. The word *inpainting*, coined by Bertalmio et al. in [3], refers to a technique whose purpose is to restore damaged portions of an image. In terms of psychology of vision inpainting corresponds to *amodal completion*, a phenomenon described by Kanizsa in [46], which consists in the completion of the occluded part of an image. This problem can be faced with many techniques such as geometric and variational instruments which start from the selection of existing boundaries or algorithms acting directly on the image space, based on the Gestalt law of good continuation and the classical findings of psychology of vision. This last class of algorithms goes back to the works of Kanizsa [46], Ullman [69], and Horn [41] and we find the prototype of models for curve completion into Mumford’s Elastica functional (see [52]):

$$\int_{\gamma} (1 + k^2) ds.$$

This expression minimizes a functional defined on the curve itself, where k is the curvature along the curve γ , parametrized by arc length s . The models proposed by Mumford, Nitzberg,

*Received by the editors March 23, 2015; accepted for publication (in revised form) October 20, 2015; published electronically February 23, 2016. This research received funding from the People Programme (Marie Curie Actions) of the European Union’s Seventh Framework Programme FP7/2007-2013 under REA grant agreement n607643.

<http://www.siam.org/journals/siims/9-1/M101357.html>

[†]Dipartimento di Matematica, Università di Bologna, Bologna 40126, Italy (giovanna.citti@unibo.it).

[‡]Center of Mathematics, CNRS-EHESS, 75244 Paris Cedex 13, France (benedetta.franceschiello@ehess.fr, alessandro.sarti@ehess.fr).

[§]Department of Mathematics and Computer Science, TUE, Eindhoven 5600 MB, Netherlands (g.r.sanguinetti@tue.nl). The research of this author received funding from the European Research Council under the Seventh Framework Programme (FP7/2007 2014)/ERC grant agreement 335555.

and Shiota (see [52] and [54]) and by Masnou and Morel (see [50]) generalize this principle to the level sets of a gray-valued image. In fact, if D is a squared defined in \mathbb{R}^2 and $I : D \rightarrow \mathbb{R}$ is an image, the considered functionals are second order functionals defined on I :

$$\int_D |\nabla I| \left(1 + \left| \operatorname{div} \left(\frac{\nabla I}{|\nabla I|} \right) \right|^2 \right) dx dy.$$

A model expressed by a system of two equations, one responsible for boundary extraction and one for figure completion, was proposed by Bertalmio et al. in [3]. In Sarti, Malladi, and Sethian [67] the role of the observer was considered, letting evolve by curvature in the Riemannian metric associated to the image a fixed surface called *point of view surface*.

Close to the completion problem there is the one of enhancement, allowing one to make the structures of images more visible while reducing the noise. For contours enhancement, models expressed as nonlinear PDEs dependent on the gradient were proposed by Nitzberg and Shiota [55] and Cottet and Germain [19]. Later on, Weickert [72, 73] proposed a coherence-enhancing diffusion method, called CED. Let us also mention the models of Tschumperlé [68], who included curvature in the diffusion process in order to improve enhancement.

A different class of algorithms for performing both completion and enhancement is directly inspired by the functionality of the visual cortex, which is expressed in terms of contact structures and Lie groups with a sub-Riemannian metric. We refer to section 2 for a precise definition of this metric and for references of the mathematical aspects of the problem. We only recall here that PDEs in this setting are totally degenerate at every point, so that classical results on PDE cannot be applied to study their solutions. Then we will follow the approach provided by Evans and Spruck in [29]. The first geometric models of the functionality of the visual cortex date back to the papers of Hoffmann [38], Koenderink and van Doorn [48], and Zucker [74]. Petitot and Tondut in [59] proposed a model of single boundaries completion through constraint minimization in a contact structure, obtaining a neural counterpart of the models of Mumford; see [52]. Sarti and Citti in [65] and [18] proposed to model the cortical structure as Lie group $SE(2)$ of rigid transformations of the plane with a sub-Riemannian metric. Each two-dimensional (2D) retinotopic image is lifted to a surface in this higher dimensional structure and processed by the long range via a diffusion driven motion by curvature. This model performs amodal completion on the whole image and can be considered the cortical counterpart of the models of Nitzberg, Mumford, and Shiota [54]. A large class of algorithms of image processing in Lie groups were developed by Duits et al. in [26]. The main instrument they developed is an invertible map from the 2D retinal image to the feature space expressed in terms of Fourier instruments. Duits et al. faced both the problem of contour completion and enhancement in the presence of crossing and bifurcating lines (see [26, 27]). We will always use the word “enhancement” with the same meaning as in their works. Let us also recall the results of Boscaïn et al. [9], who studied properties of the diffusion using a semidiscrete implementation and instruments of group Fourier transform similar to the ones proposed by Duits and Franken in [27] and obtained numerical results to the completion problem with heuristic complements.

In this paper we reconsider the sub-Riemannian cortical model of image completion introduced in [18, 65]. This model combines two mechanisms, the sub-Riemannian diffusion and the concentration, giving rise to a diffusion driven motion by curvature. In the original

paper [65, 18] the authors proved the convergence of the diffusion-concentration algorithm to the mean curvature flow, in the sense that each point of the surface moves in the direction of the normal, with speed equal to the curvature. This can be considered a local definition of mean curvature flow. If the surface is represented as a level set, the fact that each point moves as expressed before is formally expressed through a degenerate PDE, which can be considered an alternative definition of mean curvature flow. In this paper we give a formal proof of the existence of viscosity solutions of this PDE, proving that the two definitions lead to the same flow, i.e., a sub-Riemannian motion by curvature. Existence results for this type of equation in the Euclidean setting are well known (see, for example, [29]) but in the sub-Riemannian setting the existence of a solution was known only for the Heisenberg group (see [10, 30]). Here we start filling the gap, extending the existence results of [29] in the present setting. In particular we look for a sub-Riemannian viscosity solution as a limit of the analogous problem in an approximating Riemannian setting. The main difficulty we have to face is the fact that in the sub-Riemannian setting the derivatives are replaced by directional derivatives, which in general do not commute. The model had been initially developed to solve the completion problem. Here we propose to use the sub-Riemannian Laplacian also to perform enhancement of boundaries, and directional denoising. Indeed we will see that the action of the sub-Riemannian diffusion is strongly directional, and it reduces noise only in the direction of contours. Conversely, it performs no diffusion in the orthogonal direction, preserving the structures of the images.

The paper is organized as follows. In section 2 we reconsider the completion model of Sarti and Citti (see [65]) and propose to extend its application to perform contours enhancement. Since the model is formally expressed as a diffusion driven motion by curvature, in section 3 we consider the mean curvature equation in the $SE(2)$ group and prove the existence of viscosity solutions. In section 4 we discuss the numerical scheme used to implement the mean curvature flow. Finally in section 5 we conclude the paper by showing some numerical results of completion and enhancement and comparing different methods.

2. Sub-Riemannian operators in image processing. In this section we first recall the cortical model of image completion proposed by Citti and Sarti in [65] and [18]. For simplicity we will focus only on the image processing aspects of the problem, neglecting all the cortical ones. Then we show that this mechanism can be adapted to perform contours enhancement.

2.1. Processing of an image in a sub-Riemannian structure.

2.1.1. Lifting of the level lines of an image. The cortical based model of completion, proposed by Citti and Sarti in [65] and [18], lifts each level line of a 2D image $I(x, y)$ in the retinal plane to a new curve in the group $SE(2) = \mathbb{R}^2 \times S^1$ of rigid motions of the Euclidean plane, used to model the functional architecture of the primary visual cortex (V1). Precisely, up to a convolution with a Gaussian bell, we can assume that at almost for every point (x, y) in the domain of I the unitary tangent to the level lines of I is well defined:

$$\vec{X}_1 = (\cos(\bar{\theta}(x, y)), \sin(\bar{\theta}(x, y)))$$

(see also [8]). Since the normal vector field is defined a.e., the lifting in the $SE(2) = \mathbb{R}^2 \times S^1$ is well defined a.e. and represents the action of simple cells. While looking at the complex

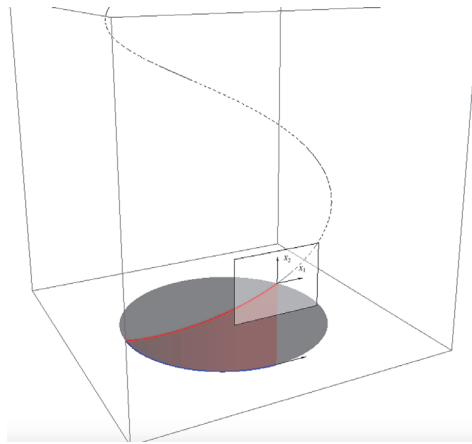


Figure 1. A contour represented by the curve $\gamma_{2D}(t)$ is lifted into the roto-translation group obtaining the red curve $\gamma_{3D}(t)$. The tangent space of the roto-translation group is spanned by the vectors X_1^0 and X_2^0 .

ones, two opposite directions are identified, and the lifting is performed in $\mathbb{R}^2 \times P^1$. Then the choice of this orientation lifts the level line $\{I(x, y) = cost\}$ to a new curve in $\mathbb{R}^2 \times S^1$ as shown in Figure 1. By construction a tangent vector to any lifted curve γ_{3D} in $SE(2)$ can be represented as a linear combination of the vector fields:

$$X_1^0 = \cos(\theta)\partial_x + \sin(\theta)\partial_y, \quad X_2^0 = \partial_\theta.$$

In other words we have associated to every point of $\mathbb{R}^2 \times S^1$ the vector space spanned by vectors X_1^0 and X_2^0 .

2.1.2. The sub-Riemannian structure. We will call the horizontal plane and denote it as HM the tangent plane generated by X_1^0 and X_2^0 at every point. Let us also note that there are no lifted curves with a nonvanishing component in the orthogonal direction

$$X_3 = -\sin(\theta)\partial_x + \cos(\theta)\partial_y.$$

In order to clarify notation, we use X_1^0, X_2^0 for the horizontal vector fields and X_3 for the nonhorizontal one. However, derivations in the direction X_3 can be recovered by means of the commutator:

$$X_3 = X_1^0 X_2^0 - X_2^0 X_1^0 = [X_1^0, X_2^0] = -\sin(\theta)\partial_x + \cos(\theta)\partial_y.$$

This condition ensures that X_1^0, X_2^0 and their commutators of any order span the tangent space of $SE(2)$ at every given point, i.e., they satisfy the Hörmander condition; see [40]. Then the structure obtained with this lifting process is sub-Riemannian. On the plane HM we define the metric g_0 which makes X_1^0 and X_2^0 orthonormal. Hence, if a vector $a = a_1 X_1^0 + a_2 X_2^0 \in HM$, its horizontal norm is

$$(1) \quad |a|_0 = \sqrt{(a_1)^2 + (a_2)^2}.$$

The first classical properties of the distance in these spaces have been established by Nagel, Stein, and Wainger (see [53]) and Gromov (see [35]). We refer to Hladky (see [36]) and the references therein for recent contributions.

In this setting the vector fields play the same role as derivatives in the standard setting. Hence we will say that a function $u : \mathbb{R}^2 \times S^1 \rightarrow \mathbb{R}$ is of class C^1 in the sub-Riemannian sense (we will denote it as $u \in C_{SR}^1$) if there exists $X_1^0 u$ and $X_2^0 u$ and they are continuous. In this case we will call horizontal gradient ∇_0

$$\nabla_0 u = (X_1^0 u)X_1^0 + (X_2^0 u)X_2^0.$$

From the definition stated before it follows that the norm of the horizontal gradient is

$$(2) \quad |\nabla_0 u| = \sqrt{(X_1^0 u)^2 + (X_2^0 u)^2}.$$

In other words the horizontal gradient is the projection of the standard gradient of u on the horizontal plane HM .

2.1.3. Lifting of the image to a regular surface. Since each level line of the image I is lifted to a curve in the 3D cortical space, the whole image is lifted to a graph

$$(x, y) \rightarrow (x, y, \bar{\theta}(x, y)).$$

Clearly the graph of θ can be interpreted as the zero level set of the function u

$$u(x, y, \theta) = \theta - \bar{\theta}(x, y),$$

and it can be identified as a regular surface in the sub-Riemannian structure. The notion of regular surface S was first introduced by Franchi, Serapioni, and Serra Cassano in [32]:

$$(3) \quad S = \{(x, y, \theta) : u(x, y, \theta) = 0 \text{ and } \nabla_0 u(x, y, \theta) \neq 0\}.$$

The horizontal normal of S is defined as

$$\nu_0 = \frac{\nabla_0 u}{|\nabla_0 u|}.$$

Note that in a smooth surface there can be points where the Riemannian gradient is not 0, but its projection on the HM plane vanishes:

$$\nabla_0 u = 0.$$

Points which have this property are called *characteristics* and the normal is not defined at them. However, these points are not present in lifted surfaces. At every point of the surface there is a unique unitary tangent vector, which is horizontal:

$$(4) \quad T_0 = \frac{(X_2^0 u, -X_1^0 u)}{|\nabla_0 u|}.$$

The integral curves of this vector field define a foliation of the surface in horizontal curves (also called Legendrian foliation—see [57], [16], [12], and [34] for the properties of these curves).

2.1.4. Diffusion and concentration algorithm. We have seen in subsection 2.1.3 how to lift an image $I(x, y)$ to a surface S . After that let us lift the level lines of the image $I(x, y)$ to the function

$$v(x, y, \bar{\theta}(x, y)) = I(x, y)$$

defined on the surface. The surface S and the function v defined on S will be processed through differential operators defined on $SE(2)$, which model the propagation of information in the cortex. More precisely two mechanisms operate on the lifted surface S :

- (a) A sub-Riemannian diffusion along the vector fields X_1^0 and X_2^0 which model the propagation of information through the cortical lateral connectivity. This operator can be expressed as

$$\partial_t - X_{11}^0 - X_{22}^0,$$

where X_{11}^0 and X_{22}^0 are the second derivative in the direction X_1^0 and X_2^0 , respectively. The operator is formally degenerated, in the sense that its second fundamental form has 0 determinant at every point. It has been deeply studied starting from the classical works of Hörmander in [39], Rothschild and Stein in [62], and Jerison [45] and it is known that it is hypoelliptic. After that a large literature has been produced on these types of operators, and we refer to [13] for a recent presentation of the state of the art.

- (b) A concentration on the surface of maxima to model the nonmaximal suppression mechanism and the orientation tuning.

In the Euclidean setting Merrimann, Bence, and Osher proved in [51] the convergence of a similar two-step algorithm to the motion by curvature. In [65] and [18] Citti and Sarti studied the motion when (a) and (b) are applied iteratively and proved that at each step the surface performs an increment in the normal direction with speed equal to the sub-Riemannian mean curvature.

2.1.5. Mean curvature flow. The notion of curvature of a C^2 surface at noncharacteristic points is already well understood (see [22, 37, 15, 61, 13]). It can be defined as the first variation of the area functional, as a limit of the mean curvature of the Riemannian approximation, or as horizontal divergence of the horizontal normal:

$$K_0 = \operatorname{div}_0(\nu_0) = \operatorname{div}_0\left(\frac{\nabla_0 u}{|\nabla_0 u|}\right).$$

We refer to the appendix for the definition of the horizontal divergence. If each point of the surface evolves in the direction of the normal vector with speed equal to the mean curvature, we say that the surface is evolving by mean curvature. From the previous expression of the curvature we formally get the following equation for the flow, which we can call the horizontal (or sub-Riemannian) mean curvature flow:

$$(5) \quad \begin{cases} u_t = \sum_{i,j=1}^2 \left(\delta_{i,j} - \frac{X_i^0 u X_j^0 u}{|\nabla_0 u|^2} \right) X_i^0 X_j^0 u & \text{in } \Omega \subset \mathbb{R}^2 \times S^1, \\ u(\cdot, 0) = u_0, \end{cases}$$

where δ_{ij} is the Kronecker function. An existence result for this equation was not known, and we will provide in the next section an existence theorem. In order to simplify notation we will denote

$$(6) \quad A_{ij}^0(\nabla_0 u) = \delta_{ij} - \frac{X_i^0 u X_j^0 u}{|\nabla_0 u|^2}, \quad i, j = 1, 2.$$

2.1.6. Laplace–Beltrami flow. Citti and Sarti also conjectured that as a result of the previous mechanisms the function $v(x, y, \bar{\theta}(x, y))$, which contains the gray level values, evolves through the flow described by the Laplace–Beltrami operator Δ_{LB} :

$$(7) \quad \begin{cases} v_t = \Delta_{LB} v, \\ v(\cdot, 0) = v_0. \end{cases}$$

This operator expresses a diffusion of the variable v on the surface level set of the variable u . The definition of the Laplace–Beltrami operator is recalled in the appendix. Let us note that the described equations become degenerate and the solutions are regular only along the directions of the foliation defined in (4)

2.2. Enhancement and inpainting in sub-Riemannian geometry.

2.2.1. Inpainting of missing parts of the image. In the previous section we described the main instruments necessary for describing the completion model of [65]. Let us recall here the proposed algorithm. As usual while restoring damaged portions of an image we assume that the corrupted set ω is known a priori.

1. An image $I(x, y)$ is lifted to a surface $S = \{(x, y, \bar{\theta}(x, y))\}$ in the Lie group $SE(2)$ of rotations and translations and the gray levels of the image $I(x, y)$ to a function $v(x, y, \bar{\theta}(x, y))$ defined on S . In the lifting the corrupted part of the image becomes $\Omega = \omega \times S^1$, where no surface is defined.
2. The surface S and $v(x, y, \bar{\theta}(x, y))$ are processed via the algorithm of diffusion and concentration in the corrupted region Ω , where we impose Dirichlet boundary conditions. This leads to the motion by mean curvature of the surface S and to a Laplace–Beltrami flow for $v(x, y, \bar{\theta}(x, y))$.
3. The final result is obtained by reprojecting onto the plane of the image the values of the intensity $v(x, y, \bar{\theta}(x, y))$.

The algorithm has been implemented in [64] via a diffusion and concentration method, while it has been implemented via the curvature equation in [65].

2.2.2. Enhancement of boundaries. Part of the scope of this paper is to extend the previous completion algorithm to solve the problem of contours enhancement. The aim of this technique is to provide a regularization in the direction of the boundaries, making them clearer and brighter and eliminating noise. We refer to the papers of Franken and Duits [28, 33] for some results of image enhancement in this space. Precisely, they lift the image I in the 3D features space, using an invertible map defined through Fourier analysis. The lifted version of the image I is processed in the 3D space and then reprojected on the 2D plane to recover an enhanced version of the image I . In particular they also provide results of enhancement in the presence of bifurcation or crossing. In this paper we face the same problem adapting the algorithm recalled in the previous section.

1. First we lift the level lines of an image $I(x, y)$ to a surface $S = \{(x, y, \bar{\theta}(x, y))\}$ and we lift the gray levels of $I(x, y)$ to a function $v(x, y, \bar{\theta}(x, y))$ always defined on S .
2. Then we process the surface S via a mean curvature flow and v via a Laplace–Beltrami flow. In order to perform enhancement we propose here to let (5) and (7) evolve in the full domain $\mathbb{R}^2 \times S^1$. Let us remark that lifting the image in the 3D group allows us to solve the problem of crossing elongated structures. Indeed if two lines cross in the 2D space and have different orientations, they are lifted to the 3D space to two different planes, allowing completion and enhancement. The directional diffusion will regularize only in the direction of contours.
3. Finally we project into the plane of the image the values of the gray intensity $v(x, y, \theta(x, y))$.

3. Existence of vanishing viscosity solutions. In this section we provide the main result of this paper, which is the proof of existence of solutions for the mean curvature flow in $SE(2)$. We explicitly note that we do not need to develop new results for the Laplace–Beltrami operator, which is linear.

As we can immediately observe the PDE becomes degenerate in the singularities of the horizontal gradient of the solution $u(\cdot, t)$. The notions of viscosity and vanishing viscosity solutions have been introduced in order to overcome this problem. The method of generalized (viscosity) solutions independently developed by Chen, Giga, and Goto [17], by Evans and Spruck [29], and by Crandall, Ishii, and Lions [20] is now applied to large classes of degenerate equations [44]. Recently it has been extended also in the sub-Riemannian setting; see [71, 10, 30]. Finally let us recall that Dirr, Dragoni, and von Renesse. [25] have recently studied a probabilistic approach to the mean curvature flow in the context of the Heisenberg group.

Here we follow the presentation of Evans and Spruck [29], who used the notion of vanishing viscosity to establish existence of a solution. Since the curvature equation is degenerate, the idea is to approximate the given equation with a uniformly elliptic one, establish results for the approximating problem, and prove that in the limit this leads an existence result for the given equation. In the last section we introduce other notions of viscosity solutions and we clarify the relation between the different definitions of solutions we have introduced.

3.1. The notion of vanishing viscosity solution. A vanishing viscosity solution is the limit of the solutions of approximating regular problems.

Let us first explicitly note that the coefficients A_{ij}^0 are degenerate: when the gradient vanishes, they are not defined. Hence we will apply the regularization procedure proposed by Evans and Spruck in [29] to face singularities, which consists in replacing the coefficients with the following ones:

$$A_{ij}^\tau(p) = \left(\delta_{ij} - \frac{p_i p_j}{|p|^2 + \tau} \right).$$

This approximation has a clear geometric interpretation, already provided by Evans and Spruck. In (5) each level set of u evolves by mean curvature. What we obtain adding a new parameter is the evolution of the graph of u

$$\Gamma_t^\tau = \{(\xi, \xi_{n+1}) \in \mathbb{R}^{n+1} | \xi_{n+1} = u(\xi, t)\}$$

and the introduction in the space of a metric depending on τ . In this approximation equation (5) reads as

$$(8) \quad \begin{cases} u_t = \sum_{i,j=1}^2 A_{ij}^\tau (\nabla_0 u) X_i^0 X_j^0 u & \text{in } \Omega \subset \mathbb{R}^2 \times S^1, \\ u(\cdot, 0) = u_0. \end{cases}$$

We will now introduce a Riemannian approximation of the mean curvature flow in the graph approximation we made before. We extend g_0 to a metric g_ϵ defined on the whole tangent space of $SE(2)$ which makes the vectors $X_1^0, X_2^0, \epsilon X_3$ orthonormal. Let us note that g_ϵ is the Riemannian completion of the horizontal metric. We will always denote

$$(9) \quad X_1^\epsilon = X_1^0, \quad X_2^\epsilon = X_2^0, \quad X_3^\epsilon = \epsilon X_3.$$

This notation justifies the choice of calling X_i^0 the sub-Riemannian vector fields: indeed they can be obtained for $\epsilon = 0$. The Riemannian gradient associated to the metric g_ϵ will be represented as

$$\nabla_\epsilon u = X_1^\epsilon u X_1^\epsilon + X_2^\epsilon u X_2^\epsilon + X_3^\epsilon u X_3^\epsilon$$

and, using the fact that X_i^ϵ are orthonormal, we get

$$(10) \quad |\nabla_\epsilon u| = \sqrt{(X_1^\epsilon u)^2 + (X_2^\epsilon u)^2 + (X_3^\epsilon u)^2}.$$

In the Riemannian setting (8) reads as

$$(11) \quad \begin{cases} u_t = \sum_{i,j=1}^3 A_{ij}^{\epsilon,\tau} (\nabla_\epsilon u) X_i^\epsilon X_j^\epsilon u & \text{in } \Omega \subset \mathbb{R}^2 \times S^1, \\ u(\cdot, 0) = u_0, \end{cases}$$

where

$$A_{ij}^{\epsilon,\tau} (\nabla_\epsilon u) = \left(\delta_{i,j} - \frac{X_i^\epsilon u X_j^\epsilon u}{|\nabla_\epsilon u|^2 + \tau} \right).$$

In order to prove the existence of a solution we apply another regularization, always introduced by Evans and Spruck. It consists in adding a Laplacian, ensuring that the matrix of the coefficients has strictly positive smallest eigenvalue. Then the approximated coefficients will be

$$A_{ij}^{\epsilon,\tau,\sigma}(p) = A_{ij}^{\epsilon,\tau}(p) + \sigma \delta_{ij}$$

and the associated equation becomes

$$(12) \quad \begin{cases} u_t = \sum_{i,j=1}^3 A_{ij}^{\epsilon,\tau,\sigma} (\nabla_\epsilon u) X_i^\epsilon X_j^\epsilon u & \text{in } \Omega \subset \mathbb{R}^2 \times S^1, \\ u(\cdot, 0) = u_0. \end{cases}$$

This condition makes the coefficients satisfy the coercivity condition and allows us to apply the standard theory of uniformly parabolic equations.

We are now in a condition to give the definition of vanishing viscosity solution.

Definition 3.1. *A function u is a vanishing viscosity solution of (5) if it is a limit of a sequence of solutions $u^{\epsilon_k, \tau_k, \sigma_k}$ of (12).*

3.2. Solution of the approximating equations. The aim of this subsection is to study the approximating equation (12). Since it is uniformly parabolic we will recognize that standard PDE results provide existence of the solution. We are here interested in establishing estimates independent of all parameters for the solution and its gradient.

Theorem 3.2. *Assume that $u_0 \in C^\infty(\mathbb{R}^2 \times S^1)$ and that it is constant on the exterior of a cylinder, i.e., there exists $S > 0$ such that*

$$(13) \quad u_0 \text{ is constant on } \mathbb{R}^2 \times S^1 \cap \{x^2 + y^2 \geq S\}.$$

Then there exists a unique solution $u^{\epsilon, \tau, \sigma} \in C^{2, \alpha}(\mathbb{R}^2 \times S^1 \times [0, \infty))$ of the initial value problem (12). Moreover, for all $t > 0$ one has

$$(14) \quad \|u^{\epsilon, \tau, \sigma}(\cdot, t)\|_{\mathcal{L}^\infty(\mathbb{R}^2 \times S^1)} \leq \|u_0\|_{\mathcal{L}^\infty(\mathbb{R}^2 \times S^1)},$$

$$(15) \quad \|\nabla_E u^{\epsilon, \tau, \sigma}(\cdot, t)\|_{\mathcal{L}^\infty(\mathbb{R}^2 \times S^1)} \leq \|\nabla_E u_0\|_{\mathcal{L}^\infty(\mathbb{R}^2 \times S^1)},$$

where $\nabla_E(\cdot)$ denotes the Euclidean gradient.

This result generalizes to $SE(2)$ the previous results of [29] and [10].

The first step of the proof of Theorem 3.2 is the existence of the function u and its L^∞ bound.

Theorem 3.3. *Under the assumption of Theorem 3.2 on the initial datum, the initial value problem (12) has a unique solution $u^{\epsilon, \tau, \sigma} \in C^{2, \alpha}(\mathbb{R}^2 \times S^1 \times [0, \infty))$ such that*

$$(16) \quad \|u^{\epsilon, \tau, \sigma}(\cdot, t)\|_{\mathcal{L}^\infty(\mathbb{R}^2 \times S^1)} \leq \|u_0\|_{\mathcal{L}^\infty(\mathbb{R}^2 \times S^1)}.$$

Proof. For $\sigma > 0$, consider the problem associated to (12) on a cylinder $B(0, r) \times [0, T]$, with initial data

$$(17) \quad u_r^{\epsilon, \tau, \sigma}(\cdot, 0) = u_0$$

and constant value on the lateral boundary of the cylinder. Note that coefficients $A_{ij}^{\epsilon, \tau, \sigma}$ satisfy the uniform parabolic condition

$$(18) \quad \sigma|p|^2 \leq A_{ij}^{\epsilon, \tau, \sigma}(\tilde{p})p_i p_j$$

for each $\tilde{p}, p \in \mathbb{R}^3$. Hence the theory of parabolic equations on bounded cylinders ensures that for every fixed value of the parameters there exists a unique smooth solution $u_r^{\epsilon, \tau, \sigma}$ (see, for example, Ladyzenskaja, Solonnikow, and Ural'ceva [49]). By the maximum principle we have

$$(19) \quad \|u_r^{\epsilon, \tau, \sigma}(\cdot, t)\|_{\mathcal{L}^\infty(\mathbb{R}^2 \times S^1)} \leq \|u_0\|_{\mathcal{L}^\infty(\mathbb{R}^2 \times S^1)}.$$

Letting r tend to ∞ , we obtain a solution $u^{\epsilon, \tau, \sigma}$ defined on the whole $\mathbb{R}^n \times [0, T]$ such that

$$\|u^{\epsilon, \tau, \sigma}\|_\infty \leq \|u_0\|_{\mathcal{L}^\infty(\mathbb{R}^2 \times S^1)}. \quad \blacksquare$$

The second step of the proof is the estimate of the gradient. In order to obtain this estimate we differentiate (12), obtaining the equation satisfied by the gradient, and we apply

the maximum principle. The main difficulty to face is the fact that the vector fields X_i^ϵ do not commute, hence it is not easy to find a nice equation satisfied by the gradient. We will take the derivatives along the direction of a family of vector fields

$$\begin{aligned} Y_1 &= \partial_x, \\ Y_2 &= \partial_\theta - y\partial_x + x\partial_y, \\ Y_3 &= \partial_y, \end{aligned}$$

which are right invariant with respect to the group law. These vector fields are widely used: Mumford in [52] used them for a different purpose. In particular it is well known that these vector fields commute with the left invariant ones X_i^ϵ .

Let us start directly verifying that the vector fields (X_i^ϵ) and (Y_i) commute.

Lemma 3.4. *The vector fields $\{X_i^\epsilon\}_{i=1,2,3}$ defined in (9) commute with $\{Y_i\}_{i=1,2,3}$, just defined.*

Proof. We calculate their Lie bracket:

$$\begin{aligned} [X_1^0, Y_1] &= (\cos \theta \partial_x + \sin \theta \partial_y) \partial_x - \partial_x (\cos \theta \partial_x + \sin \theta \partial_y) \\ &= \cos \theta \partial_{xx} + \sin \theta \partial_{yx} - \cos \theta \partial_{xx} - \sin \theta \partial_{xy} = 0. \end{aligned}$$

Since the coefficients of Y_2 do not depend on θ it is clear that

$$[X_2^0, Y_2] = 0.$$

Finally

$$\begin{aligned} [X_3, Y_3] &= (\sin \theta \partial_x - \cos \theta \partial_y) \partial_y - \partial_y (\sin \theta \partial_x - \cos \theta \partial_y) \\ &= \sin \theta \partial_{xy} - \cos \theta \partial_{yy} - \sin \theta \partial_{xy} + \cos \theta \partial_{yy} = 0. \end{aligned}$$

The other combinations can be analogously computed. ■

We can now obtain the estimate of the gradient.

Theorem 3.5. *Under the assumption of Theorems 3.2 and 3.3, the solution of the initial value problem (12) satisfies*

$$(20) \quad \|\nabla_E u^{\epsilon, \tau, \sigma}(\cdot, t)\|_{\mathcal{L}^\infty(\mathbb{R}^2 \times S^1)} \leq \|\nabla_E u_0\|_{\mathcal{L}^\infty(\mathbb{R}^2 \times S^1)}.$$

Proof. From Theorem 3.3 we know that there exists a unique smooth solution $u^{\epsilon, \tau, \sigma}$ of (12) and we only have to estimate its gradient. To this end, we can differentiate (12) along the directions $\{Y_i\}_{i=1,2,3}$, and using Lemma 3.4, we obtain the following equation for $w_i = Y_i u^{\epsilon, \tau, \sigma}$, for all $i = 1, 2, 3$, and for $\omega_4 = Y_2 u^{\epsilon, \tau, \sigma} - (y_0 \partial_x - x_0 \partial_y) u^{\epsilon, \tau, \sigma}$ (for every fixed value (x_0, y_0)):

$$(21) \quad \frac{\partial}{\partial t} w_i = \sum_{i,j,k=1}^3 \left(A_{i,j}^{\epsilon, \tau, \sigma} (\nabla_\epsilon u^{\epsilon, \tau, \sigma}) X_i^\epsilon X_j^\epsilon w_i + (\partial_{\xi_k} A_{i,j}^{\epsilon, \tau, \sigma}) (\nabla_\epsilon u^{\epsilon, \tau, \sigma}) X_i^\epsilon X_j^\epsilon u^{\epsilon, \tau, \sigma} X_k^\epsilon w_i \right).$$

The parabolic maximum principle applied to the previous equation yields

$$(22) \quad \|Y_i u^{\epsilon, \tau, \sigma}(\cdot, t)\|_{\mathcal{L}^\infty(\mathbb{R}^2 \times S^1)} \leq \|Y_i u_0\|_{\mathcal{L}^\infty(\mathbb{R}^2 \times S^1)}.$$

This implies that

$$\|\partial_x u^{\epsilon, \tau, \sigma}(\cdot, t)\|_{\mathcal{L}^\infty(\mathbb{R}^2 \times S^1)} + \|\partial_y u^{\epsilon, \tau, \sigma}(\cdot, t)\|_{\mathcal{L}^\infty(\mathbb{R}^2 \times S^1)} \leq C \|\nabla_E u_0\|_{\mathcal{L}^\infty(\mathbb{R}^2 \times S^1)}.$$

Now we have to establish the estimate of the derivative ∂_θ . For every fixed value of (x_0, y_0) we have

$$\begin{aligned} |\partial_\theta u^{\epsilon, \tau, \sigma}(x_0, y_0, \theta)| &\leq \max_{|y-y_0|^2+|x_0-x|^2 \leq 1} |Y_2 u^{\epsilon, \tau, \sigma} - (y_0 \partial_x - x_0 \partial_y) u^{\epsilon, \tau, \sigma}| \\ &\leq \max_{|y-y_0|^2+|x_0-x|^2 \leq 1} |Y_2 u_0 - (y_0 \partial_x - x_0 \partial_y) u_0| \\ &\leq \max_{|y-y_0|^2+|x_0-x|^2 \leq 1} |\partial_\theta u_0| + \max_{|y-y_0|^2+|x_0-x|^2 \leq 1} |y_0 - y| |\partial_x u_0| + \max_{|y-y_0|^2+|x_0-x|^2 \leq 1} |x_0 - x| |\partial_y u_0| \\ &\leq \|\nabla_E u_0\|_{\mathcal{L}^\infty(\mathbb{R}^2 \times S^1)}. \quad \blacksquare \end{aligned}$$

Let us conclude this section by remarking that the proof of Theorem 3.2 is a direct consequence of Theorems 3.3 and 3.5.

3.3. Existence for the sub-Riemannian mean curvature equation. In order to extend to our setting Evans and Spruck’s argument in the proof of [29], as well as the proof of [10], we need to let the three approximating parameters $\sigma \rightarrow 0$, $\tau \rightarrow 0$, and $\epsilon \rightarrow 0$ go to 0. Since the estimates we have established are uniform in all parameters, we immediately have the existence of a vanishing viscosity solution.

Theorem 3.6. *Assume that $u_0 \in C(\mathbb{R}^2 \times S^1)$ is Lipschitz continuous and satisfies (13). Then there exists a vanishing viscosity solution $u \in C^{1,0}$ of (5), which satisfies the following properties:*

$$(23) \quad \|u(\cdot, t)\|_{\mathcal{L}^\infty(\mathbb{R}^2 \times S^1)} \leq C \|u_0\|_{\mathcal{L}^\infty(\mathbb{R}^2 \times S^1)},$$

$$(24) \quad \|\nabla_E u(\cdot, t)\|_{\mathcal{L}^\infty(\mathbb{R}^2 \times S^1)} \leq C \|\nabla_E u_0\|_{\mathcal{L}^\infty(\mathbb{R}^2 \times S^1)}.$$

Proof. Since u_0 is constant at infinity, we immediately deduce from the Weierstrass theorem that the Euclidean gradient $\nabla_E u_0$ is bounded. Employing estimates (14), (15) and the Ascoli–Arzelà theorem we can extract two sequences $\{\sigma_k\}, \{\epsilon_k\}, \{\tau_k\} \rightarrow 0$ of positive numbers such that $\frac{\epsilon_k}{\tau_k} \rightarrow 0$ and such that the corresponding solutions $\{u^k = u^{\epsilon_k, \tau_k, \sigma_k}\}_{k \in \mathbb{N}}$ are convergent in the space of Lipschitz functions. Then by definition the limit is a Lipschitz continuous vanishing viscosity solution. \blacksquare

Remark 1. Here we prove that solutions are uniformly Lipschitz continuous. Even in the Euclidean setting this is the best regularity result for solutions of equations expressed as level sets, due to the degeneracy of the equation. Only in the special case of motion by curvature of graphs can higher regularity be obtained (see, for example, Capogna, Citti, and Manfredini [11]).

3.4. Other notions of viscosity solution.

3.4.1. Viscosity solutions in the sense of jet spaces. The cortical model previously discussed associates to each planar curve γ_{2D} its orientation. This procedure can be considered as a lifting of the initial image $I(x, y)$ to a new function u defined in the space $\mathbb{R}^2 \times S^1$ of positions and orientations. We refer to Petitot and Tondut, who first described the analogous cortical process as a lifting in a jet space [59]. Another lifting process can be obtained if we associate to each function $u : \mathbb{R}^2 \times S^1 \rightarrow \mathbb{R}$ its derivatives. In this way a function u is lifted into a jet space which contains the formal analogues of its sub-Riemannian gradient $\nabla_0 u$ and the formal analogue of the elements of its horizontal Hessian matrix $X_i^0 X_j^0$ (please refer to the appendix for the definition of the horizontal Hessian). The definition of viscosity solution in jet spaces has been introduced in [20] and is now widely used in the sub-Riemannian setting (see, for example, [6]). It is based on the Taylor expansion, expressed in terms of these differential objects. The analogue of the increment in the direction of the gradient p is expressed through the notion of an exponential map (see the appendix for its precise definition), and then the increment from a point ξ in the direction $\sum_{i=1}^2 \eta_i X_i^0$ is expressed as

$$u \left(\exp \left(\sum_{i=1}^2 \eta_i X_i^0 \right) (\xi), t + s \right) - u(\xi, t).$$

At nonregular points, such as kinks, there is neither a unique vector p which identifies the horizontal gradient nor a unique matrix r_{ij} which identifies the horizontal Hessian. Hence we need to give a more general notion. If $p_i, i = 1, 2$ denotes a horizontal vector, (r_{ij}) a 2×2 matrix, and q a real number, the triplet (p, r, q) is an element of the superjet \mathcal{J}^+ for u if it satisfies the following formal analogue of the Taylor development:

$$(25) \quad u \left(\exp \left(\sum_{i=1}^2 \eta_i X_i^0 \right) (\xi), t + s \right) - u(\xi, t) \leq \sum_{i=1}^2 p_i \eta_i + \frac{1}{2} \sum_{i,j=1}^2 r_{ij} \eta_i \eta_j + qs + o(|\eta|^2 + s^2).$$

Let us note that if the super jet exists it can be used in place of the derivatives; furthermore a function u is a jet space viscosity solution if the differential equation in which the derivatives are replaced with the elements of the superjet is satisfied. More precisely, we have the following.

Definition 3.7. *A function $u \in C(\mathbb{R}^2 \times S^1 \times [0, \infty)) \cap \mathcal{L}^\infty(\mathbb{R}^2 \times S^1 \times [0, \infty))$ is a jet space-viscosity subsolution of (5) if for every (p, r, q) in the super jet we have*

$$(26) \quad q \leq \begin{cases} \sum_{i,j=1}^2 A_{ij}^0(p) r_{ij} & \text{if } |p| \neq 0, \\ \sum_{i,j=1}^2 A_{ij}^0(\tilde{p}) r_{ij} & \text{for some } |\tilde{p}| \leq 1, \text{ if } |p| = 0. \end{cases}$$

An analogous definition is provided for a viscosity supersolution. Then a viscosity solution is a function which is both a subsolution and a supersolution.

3.4.2. Viscosity solutions via test functions. The definition of viscosity solution in a jet space of a second order equation can be identified as the approximation of the solution u via a second order polynomial, whose coefficients are exactly the elements (p, r, q) of the jet

space. The definition of viscosity solution via test functions is similar, but it estimates the given solution using smooth functions instead of polynomials alone. This definition imposes the behavior of the function u at points where $u - \phi$ attains a maximum. At such points u and ϕ will have the same first derivatives, so that $\nabla_0\phi$ results to be an exact evaluation of the approximation of ∇_0u . Looking at second derivatives, it follows that for every i we have

$$X_i^0 X_i^0(u - \phi) \leq 0,$$

so that the curvature of ϕ is an upper bound for the curvature of u . Due to this observation we can give the following definition.

Definition 3.8. *A function $u \in C(\mathbb{R}^2 \times S^1 \times [0, \infty))$ is a viscosity subsolution of (5) in $\mathbb{R}^2 \times S^1 \times [0, \infty)$ if for any (ξ, t) in $\mathbb{R}^2 \times S^1 \times [0, \infty)$ and any function $\phi \in C(\mathbb{R}^2 \times S^1 \times [0, \infty))$ such that $u - \phi$ has a local maximum at (ξ, t) it satisfies*

$$(27) \quad \partial_t \phi \leq \begin{cases} \sum_{i,j=1}^2 A_{ij}^0(\nabla_0\phi) X_i^0 X_j^0 \phi & \text{if } |\nabla_0\phi| \neq 0, \\ \sum_{i,j=1}^2 A_{ij}^0(\tilde{p}) X_i^0 X_j^0 \phi & \text{for some } \tilde{p} \in \mathbb{R}^2, |\tilde{p}| \neq 1, \text{ if } |\nabla_0\phi| = 0. \end{cases}$$

A function $u \in C(\mathbb{R}^2 \times S^1 \times [0, \infty))$ is a viscosity supersolution of (5) if

$$(28) \quad \partial_t \phi \geq \begin{cases} \sum_{i,j=1}^2 A_{ij}^0(\nabla_0\phi) X_i^0 X_j^0 \phi & \text{if } |\nabla_0\phi| \neq 0, \\ \sum_{i,j=1}^2 A_{ij}^0(\tilde{p}) X_i^0 X_j^0 \phi & \text{for some } \tilde{p} \in \mathbb{R}^2, |\tilde{p}| \neq 1, \text{ if } |\nabla_0\phi| = 0. \end{cases}$$

Definition 3.9. *A viscosity solution of (5) is a function u which is both a viscosity subsolution and a viscosity supersolution.*

3.4.3. Relation between the different notions of solutions.

Theorem 3.10. *The two definitions of jet spaces viscosity solution and viscosity solution are equivalent.*

We refer to [6], where the analogous result has been proved in the Heisenberg setting. Since the result is local, it carries out also in the present setting. We will now prove that a vanishing viscosity solution is indeed a viscosity solution.

Theorem 3.11. *Assume that $u_0 \in C(\mathbb{R}^2 \times S^1)$ is continuous and satisfies (13). Then the vanishing viscosity solution detected in Theorem 3.6 is a viscosity solution $u \in C^{1,0}$ of (5).*

Proof. In order to prove that u is a viscosity solution we consider a function $\phi \in C^\infty(\mathbb{R}^2 \times S^1 \times [0, \infty))$ and we suppose that $u - \phi$ has a strict local maximum at a point $(\xi_0, t_0) \in \mathbb{R}^2 \times S^1 \times [0, \infty)$. Since u is a Lipschitz continuous vanishing viscosity solution, it can be uniformly approximated by solutions (u^k) of the approximating Riemannian problem (see also Theorem 3.11). As $u^k \rightarrow u$ uniformly near (ξ_0, t_0) , $u^k - \phi$ has a local maximum at a point (ξ_k, t_k) , with

$$(29) \quad (\xi_k, t_k) \rightarrow (\xi_0, t_0) \quad \text{as } k \rightarrow \infty.$$

Since u^k and ϕ are smooth, we have

$$\nabla_E u^k = \nabla_E \phi, \quad \partial_t u^k = \partial_t \phi \quad \text{and} \quad D_E^2(u^k - \phi) \leq 0 \quad \text{at } (\xi_k, t_k),$$

where D_E^2 is the Euclidean Hessian. Thus

$$(30) \quad \partial_t \phi - \left(\delta_{ij} - \frac{X_i^{\epsilon_k} \phi X_j^{\epsilon_k} \phi}{|\nabla_{\epsilon_k} \phi|^2 + \tau_k^2} \right) X_i^{\epsilon_k} X_j^{\epsilon_k} \phi \leq 0 \text{ at } (\xi_k, t_k).$$

This inequality can be equivalently expressed in terms of the coefficients $A_{i,j}^{\epsilon,\tau}$ as follows. At the point (ξ_k, t_k)

$$(31) \quad \partial_t \phi - A_{i,j}^{\epsilon_k, \tau_k} (\nabla_{\epsilon_k} \phi) X_i^{\epsilon_k} X_j^{\epsilon_k} \phi$$

$$(32) \quad \leq \partial_t u^k - A_{i,j}^{\epsilon_k, \tau_k} (\nabla_{\epsilon_k} u^k) X_i^{\epsilon_k} X_j^{\epsilon_k} (u^k + \phi - u^k) \leq 0.$$

If $\nabla_0 \phi(\xi_0, t_0) \neq 0$, also $\nabla_0 \phi(\xi_k, t_k) \neq 0$ for sufficiently large k . Then letting $k \rightarrow \infty$ we obtain from (32)

$$(33) \quad \partial_t \phi \leq \sum_{i,j=1}^2 \left(\delta_{ij} - \frac{X_i^0 \phi X_j^0 \phi}{|\nabla_0 \phi|^2} \right) X_i^0 X_j^0 \phi \text{ at } (\xi_0, t_0),$$

which implies that u is a viscosity subsolution.

If $\nabla_0 \phi(\xi_0, t_0) = 0$, then we set

$$\eta^k = \frac{\nabla_{\epsilon_k} \phi(\xi_k, t_k)}{\sqrt{|\nabla_{\epsilon_k} \phi(\xi_k, t_k)|^2 + \tau_k^2}}.$$

There exists $\eta \in \mathbb{R}^3$ such that $\eta^k \rightarrow \eta$. Note that

$$|(\eta^k)_3| = \frac{\epsilon_k |X_3 \phi(\xi_k, t_k)|}{\sqrt{|\nabla_{\epsilon_k} \phi(\xi_k, t_k)|^2 + \tau_k^2}} \leq \frac{(\epsilon_k / \tau_k) |X_3 \phi(\xi_k, t_k)|}{\sqrt{(\epsilon_k / \tau_k)^2 \sum_{i=1}^2 (X_i^0 \phi(\xi_k, t_k))^2 + 1}}.$$

Since the expression vanishes as $k \rightarrow \infty$ we have $\eta_3 = 0$. The PDE (32) now reads as

$$\partial_t \phi(\xi_k, t_k) - \sum_{i,j=1}^3 (\delta_{ij} - \eta_i^k \eta_j^k) X_i^{\epsilon_k} X_j^{\epsilon_k} \phi(\xi_k, t_k) \leq 0$$

so as $k \rightarrow \infty$ we obtain

$$(34) \quad \partial_t \phi(\xi_0, t_0) \leq \sum_{i,j=1}^2 (\delta_{ij} - \eta_i \eta_j) X_i^0 X_j^0 \phi(\xi_0, t_0),$$

concluding the proof for the case in which $u - \phi$ has a local strict maximum at point (ξ_0, t_0) . If $u - \phi$ has a local maximum, but not necessarily a strict local maximum at (ξ_0, t_0) , we can repeat the argument above replacing $\phi(x, t)$ with

$$\tilde{\phi}(\xi, t) = \phi(\xi, t) + |\xi - \xi_0|^4 + (t - t_0)^4$$

again to obtain (33), (34). Consequently u is a weak subsolution. That u is a weak supersolution follows analogously. ■

From the above result we can only say that there is a subsequence of $u^{\epsilon, \tau, \sigma}$ which is convergent to the vanishing viscosity solution u . In order to prove the uniqueness of the vanishing viscosity solution, we would need the sub-Riemannian analogue of the estimate established by Deckelnick and Dziuk in [24].

Proposition 3.12. *There exists a constant $C > 0$ independent of σ, τ , and ϵ such that*

$$(35) \quad \|u^{\epsilon, \tau, \sigma} - u\|_{\infty} \leq C\tau^{\alpha}.$$

Letting ϵ and σ go to 0 we also get

$$(36) \quad \|u^{\tau} - u\|_{\infty} \leq C\tau^{\alpha},$$

where u^{τ} is a solution of (8).

4. Numerical scheme. In this part we provide the numerical approximation we used to implement the sub-Riemannian motion by curvature which performs inpainting and enhancement. Since our scheme is directly inspired by the classical one of Osher and Sethian (see [56]), we will explain how to adapt the discretization to the sub-Riemannian setting. The mean curvature flow (8) can be explicitly written as

$$(37) \quad u_t = \frac{(X_2^0(u))^2 \cdot X_{11}^0(u) + (X_1^0(u))^2 \cdot X_{22}^0(u) - X_1^0(u)X_2^0(u) \cdot 2X_{12}^0(u)}{(X_1^0(u))^2 + (X_2^0(u))^2 + \tau} + \frac{X_1^0(u)X_2^0(u) \cdot [X_1^0, X_2^0](u)}{(X_1^0(u))^2 + (X_2^0(u))^2 + \tau}.$$

This equation presents two distinct terms: the first part of the flow presents second order derivatives and corresponds to the curvature term, and the second has only first order derivatives and corresponds to the metric connection. The solution $u(x, y, \theta, t)$ is discretized on a regular grid with points $x_i = i\Delta x, y_j = j\Delta y, \theta_k = k\Delta\theta$, with time discretization $t_s = s\Delta t$. We will denote $D^{+x}U(i, j, k, s), D^{-x}U(i, j, k, s), D^{0x}U(i, j, k, s)$ the forward, backward, and central difference of a discrete function U at point (i, j, k, s) with respect to x and use analogous notation for the other variables y and θ . In terms of these derivatives we will define the analogous differences in the direction of the vector fields X_1^0 and X_2^0 . Precisely if we have discretized the direction θ with K points, we will denote $\theta_k = k\pi/K$ for $k = 1, \dots, K$, and we will call

$$D^{+X_1}U(i, j, k, s) = \cos \theta_k D^{+x}U(i, j, k, s) + \sin \theta_k D^{+y}U(i, j, k, s)$$

and analogously define backward and central difference D^{-X_1}, D^{0X_1} for the vector X_1^0 and for the vector X_2^0 . Let us adapt the scheme proposed by Osher and Sethian in [56] to our case:

- (i) The first order term $X_1^0(u)X_2^0(u) \cdot [X_1^0, X_2^0](u)$ is discretized using the upwind scheme for $[X_1^0, X_2^0] = X_3$. Taking into account the upwind scheme for the vector field X_3 , the first order term is given by

$$(38) \quad W^1(U) = -\frac{\max(-\sin \theta_k D^{0X_1}U D^{0X_2}U, 0) D^{-x}U + \min(-\sin \theta_k D^{0X_1}U D^{0X_2}U, 0) D^{+x}U}{|D^{0X_1}U|^2 + |D^{0X_2}U|^2 + \tau} - \frac{\max(\cos \theta_k D^{0X_1}U D^{0X_2}U, 0) D^{-y}U + \min(\cos \theta_k D^{0X_1}U D^{0X_2}U, 0) D^{+y}U}{|D^{0X_1}U|^2 + |D^{0X_2}U|^2 + \tau}.$$

- (ii) Second order derivatives are implemented as usual as $D^{-X_1}D^{+X_1}$, $D^{-X_2}D^{+X_2}$, $D^{0X_1}D^{0X_2}$, which lead to the second order central finite difference. We will implement as central differences the first derivative coefficients of $D^{-X_1}D^{+X_1}$, $D^{-X_2}D^{+X_2}$. The first derivative with respect to X_1^0 , coefficient of the second mixed derivative, will be upwinded as before. Generalizing an idea of [14], the denominator will be a mean of central derivatives:

$$\begin{aligned} & |D_{int}U|^2(i, j, k, s) + \tau \\ &= \frac{1}{3} \sum_{k_1 \in \{k-1, k, k+1\}} |D^{0X_1}U|^2(i, j, k_1, s) + \frac{1}{5} \sum_{i_1 \in I} |D^{0X_2}U|^2(i_1, j_1, k, s) + \tau, \end{aligned}$$

where I is the family of indices $I = \{(i - 1, j), (i, j), (i + 1, j), (i, j - 1), (i, j + 1)\}$.

The second order discretized operator will be denoted $W^2(U)(i, j, k, s)$.

The difference equation associated to the continuous equation (37) will be expressed as

$$U(i, j, k, s + 1) = U(i, j, k, s) + \Delta t(W^2U)(i, j, k, s) + \Delta t(W^1U)(i, j, k, s)$$

with initial condition $U(., 0) = U_0$. We recall that convergence of difference schemes for the mean curvature flow inspired by the scheme of Osher and Sethian has been object of a large number of papers in the Euclidean setting. The stability of one of them was proved in [14]. Another monotone scheme was proposed by Crandall and Lions (see [21]) and its convergence was proved by Deckelnick in [23] and Deckelnick and Dziuk in [24].

The ideas at the basis of the stability proof of [14] can be extended to the present version of the Osher and Sethian scheme, leading to the following result.

Theorem 4.1. *The difference scheme presented above is stable in the sense that if $\Delta t \leq \frac{h^2}{10}$, then*

$$\|U\|_\infty \leq \|U_0\|_\infty.$$

Proof. If U is a solution of the discrete equation, also $V = U - \|U_0\|_\infty$ is a solution of the same equation:

$$V(i, j, k, s + 1) = V(i, j, k, s) + \Delta t(W^2V)(i, j, k, s) + \Delta t(W^1V)(i, j, k, s).$$

Hence $V(0) \leq 0$, and we have to prove $V \leq 0$, for all time. In order to study the term $W^1(V)$ we have to discuss the sign of $a_1 = -\sin \theta_k D^{0X_1}V D^{0X_2}V$ and $a_2 = \cos \theta_k D^{0X_1}V D^{0X_2}V$: we will assume that they are both positive since the proof is similar in all the other cases. In this case

$$\begin{aligned} (W^1V)(i, j, k, s) &= -\frac{a_1(V(i, j, k, s) - V(i - 1, j, k, s)) + a_2(V(i, j, k, s) - V(i, j - 1, k, s))}{|D^{0X_1}V|^2 + |D^{0X_2}V|^2 + \tau} \\ &\leq -\frac{(\cos(\theta_k) - \sin(\theta_k))D^{0X_1}V(i, j, k, s)D^{0X_2}V(i, j, k, s)}{(|D^{0X_1}V|^2 + |D^{0X_2}V|^2 + \tau)h^2}V(i, j, k, s) \leq -\frac{V(i, j, k, s)}{2h^2}. \end{aligned}$$

Analogously, having upwinded the coefficient of $(W^2V)(i, j, k, s)$, we get a similar behavior. The mixed derivatives term can be estimated as

$$-\frac{2 \cos \theta_k D^{0X_1}(D^{0X_2}V)D^{0X_2}V}{|D_{int}V|^2 + \tau}V(i, j, k, s) \leq -\frac{10V(i, j, k, s)}{h^2}.$$

In conclusion

$$V(i, j, k, s + 1) \leq V(i, j, k, s) \left(1 - \frac{10\Delta t}{h^2} \right) \leq 0.$$

The assertion then follows by induction. \blacksquare

Now we recall that the equation is uniformly parabolic in the subelliptic sense. Arguing as in [24] the estimates of fourth order derivatives can be reduced to the estimates of graphs over the considered group. Hence estimates can be obtained by a recent result of Capogna, Citti, and Manfredini (see [11]). Since for τ fixed the equation is uniformly parabolic in the subelliptic sense, these estimates allow us to prove the following.

Theorem 4.2. *If u^τ is the solution of (8) with initial condition u_0 and U is the solution of the discrete scheme considered here and α is fixed, there exist a constant $C = C(\tau, h, \alpha)$ such that if $\Delta t \leq C(\tau, h)$, then*

$$|u^\tau(i\Delta x, j\Delta y, k\Delta\theta, s\Delta t) - U(i, j, k, s)| \leq \tau^\alpha.$$

As a consequence, applying the uniqueness Theorem 3.12, we deduce the following convergence result for the solution of the mean curvature equation (5) with initial condition u_0 :

$$|u(i\Delta x, j\Delta y, k\Delta\theta, s\Delta t) - U(i, j, k, s)| \leq \tau^\alpha$$

as $\Delta t \leq C(\tau, h)$.

5. Results. In this section we present and discuss our results. We first compare the results obtained with the original algorithm [18] with some results recently appearing in the literature. Results of our new model for enhancement are proposed and compared with previous results of Duits and Franken [28].

Finally we show examples of inpainting and enhancement of images.

5.1. Inpainting results. In all the upcoming numerical experiments we have discretized the angular coordinate θ in 32 different orientations (see section 4). The evolution time (or equivalently the number of iterations of the discrete versions) for both the mean curvature flow (5) and the Laplace–Beltrami flow (7) have been set long enough so that a steady solution is ensured.

Our algorithm performs particularly well for completing gray level images which have nonvanishing gradient at every point. We start with a couple of images already contained in [64]: an artificial one (see Figure 2) and a natural one (see Figure 3). In both images a very big black hole is present, and the algorithm correctly reconstructs the missing part of the image.

Recently Boscaïn et al. in [9] tried to replace this nonlinear equation by a diffusion followed by a “heuristic complement.” In Figure 4, left, we consider an image courtesy of Boscaïn et al. [9] partially occluded by a grid: first we show the results of completion performed in [9] (second image from left), then the results obtained through the heat equation in the 2D space (third image from left), and finally the ones obtained with, Citti and Sarti model (right). A detail is shown in Figure 5. Since the considered image is a painting, extremely smooth, with low contrast, the 2D heat equation is able to perform a simple version of completion (see for example, [4]). The curvature model reconstructs correctly the missed contours and level lines and presents a strong completion capability, absent in the other two methods.

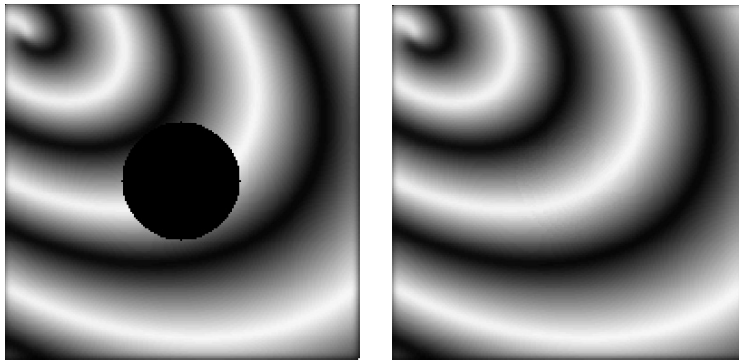


Figure 2. An example of completion performed by the algorithm. In this artificial image the image gradient is lifted in the $\mathbb{R}^2 \times S^1$ space and the black hole is completed by mean curvature flow. Since the level lines of the image are approximately circular, the algorithm performs very well.



Figure 3. Completion result on a real image through sub-Riemannian mean curvature flow in $\mathbb{R}^2 \times S^1$, as described in the paper.

In Figure 6 (and in the detail taken from it in Figure 7) we consider another example taken from the same paper. In this image the grid of points which are missing is larger, and the previous effect is even more evident.

In a more recent paper Prandi et al. (see [60]) introduced a linear diffusion with coefficients depending on the gradient of the initial image, which they call “heuristic.” In Figure 8 we compare the results obtained with this model, with the heat equation on the image plane, and with the strongly geometric model of Citti and Sarti.

Then we test our implementation on piecewise constant images. Since the gradient is 0 in a large part of the image, the lifted gradient is not defined in the largest part of the image. On the other side, since the lifting mimics the behavior of the simple cells of the V1 cortical layer, the Citti and Sarti algorithm is always applied on a smoothed version of the image. We have applied it on a classical toy problem proposed, for example, in [3] by Bertalmio, et al. Results are shown in Figure 9.

In Figure 10 we test our method on an image taken from the survey [4]. The present reconstruction is correct in the part of the image characterized by strong boundaries, but the results of [4] obtained with the model of Masnou and Morel (see [50]) seem to be better. The

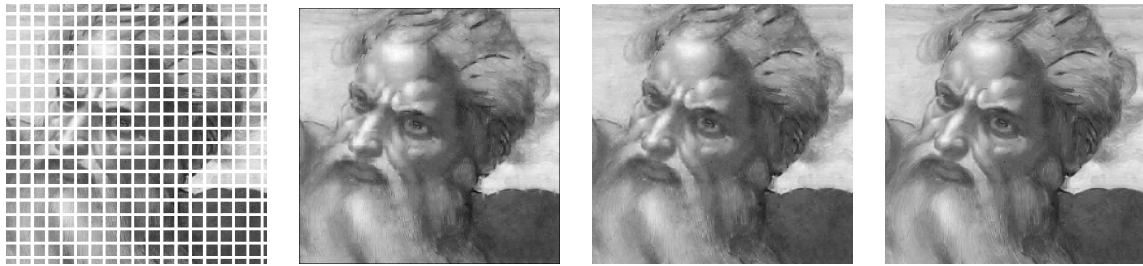


Figure 4. Left: an occluded image (courtesy of Boscain et al. [9]). Second image from left: the image processed in [9]. Third image from left: the same image processed through the heat equation. Right: the image inpainted using the Citti and Sarti algorithm.



Figure 5. A detail of the previous image. Left: the original image (courtesy of Boscain [9]). Second image from left: the image processed in [9]. Third image from left: the image processed through the heat equation; Right: the image inpainted using the proposed algorithm.

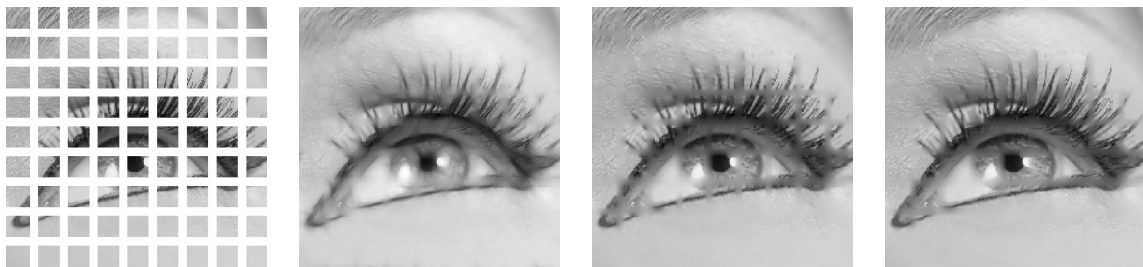


Figure 6. From left to right: the original image (courtesy of Boscain [9]); the image processed in [9]; the image processed through the heat equation; and the image inpainted using the proposed algorithm.

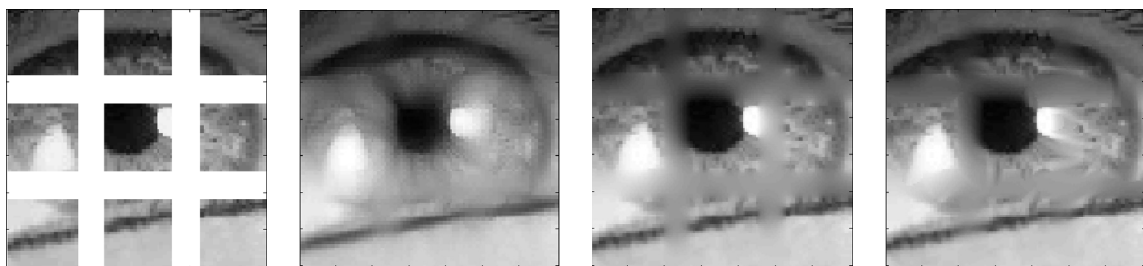


Figure 7. A detail of the previous image. Left: the original image (courtesy of Boscain [9]). Second image from left: the image processed in [9]. Third image from left: the image processed through the heat equation. Right: image inpainted using the original algorithm of Citti and Sarti.



Figure 8. On the left, the occluded image. From left to right: results from [60], with 2D heat equation and our model.

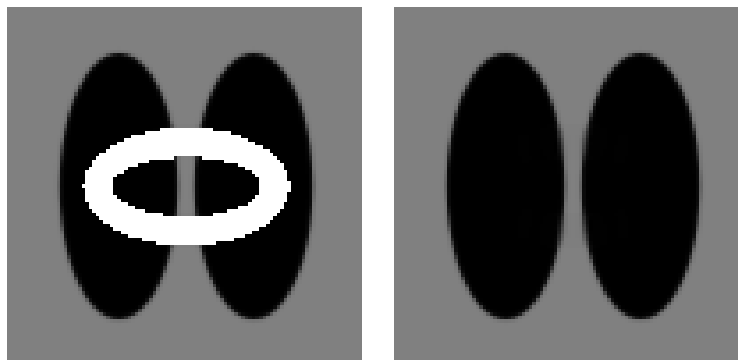


Figure 9. Inpainting a constant coefficient image with the Sarti and Citti algorithm.

main point is the boundary detection, which is very accurate in the model of Masnou and Morel, while here the boundaries are detected with a gradient, after smoothing the image.

5.2. Enhancement results. We will show in this section results of the application of the enhancement method we have introduced in section 2.2.2. Let us recall that enhancement consists in an image filtering that underlines directional coherent structures. With respect to the completion problem there is no part of the image to be disoccluded and all the parts of the initial data are evolved.

Figure 11 shows a microscopy image of bone tissue to be filtered to reconstruct the crossing fibers (courtesy of Duits and Franken [28]). The second image from the left shows the enhancement computed by using CED-OS (see [28, 33]), while the third image shows the result obtained using the proposed method.

Finally, we show in Figure 12 (zoomed in Figure 13) an example combining the techniques of completion and enhancement. We see in this case that enhancement homogenizes the original nonoccluded part with the reconstructed one.

Here we propose a detail of the previous image in order to underline the effects of the discussed techniques.

6. Conclusions. In this paper we have proved existence of viscosity solutions of the mean curvature flow PDE in $\mathbb{R}^2 \times S^1$ equipped with a sub-Riemannian metric. The flow has been



Figure 10. *Left: the occluded image. Center: image from [4] processed with the model of [50]. Right: image processed with our model.*

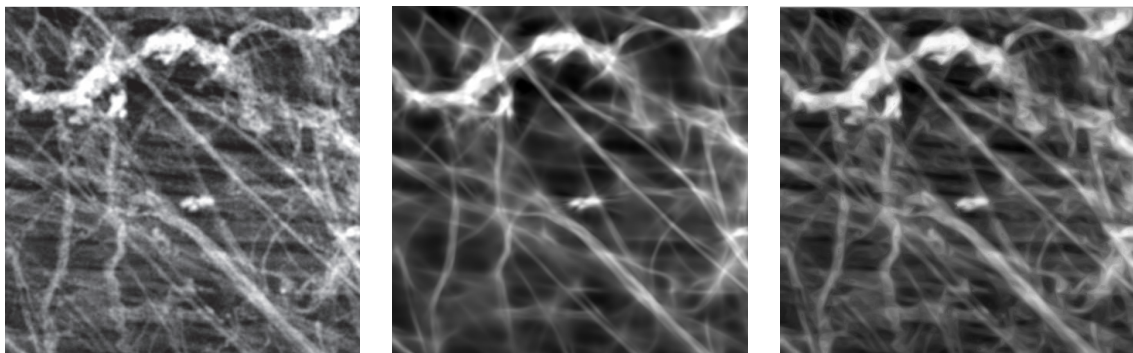


Figure 11. *From left to right: the original image, courtesy of Duits and Franken [28, Figure 7]; the enhanced image using CED-OS, (see [28]); the enhanced image obtained using the proposed method.*

implemented with a suitable adaptation of the Osher and Sethian technique [56], and a sketch of the proof of convergence of the numerical scheme is provided. Results of completion and enhancement are obtained on both artificial and natural images. We also provide comparisons with other existing algorithms. The algorithm leads to results comparable with the classical ones of Bertalmio et al. in [3] or of Masnou and Morel in [50], but it performs much better than the results shown by Boscain et al. in [9] or by Prandi et al. [60]. The method can be applied in the presence of crossing edges and to perform enhancement: our results have been compared with the previous results of Duits et al. [26].

Appendix. Here we recall the definition of the sub-Riemannian differential operators used in our paper. In the simplified setting of this group each vector field is formally self-adjoint and the vector fields are orthonormal. This allows us to give very simple definitions where the vector fields take the place of the derivatives in the standard setting.

Definition A.1 (horizontal Hessian). *The horizontal Hessian of a function f is defined as*

$$H_f = (X_i^0 X_j^0(f) + X_j^0 X_i^0(f))_{i,j=1,2},$$

i.e., is the matrix which contains the second order derivatives of the horizontal vector fields.



Figure 12. Left: the original image (courtesy of Boscain et al. [9]). Center: image inpainted using the proposed algorithm. Right: image inpainted and enhanced with this algorithm.

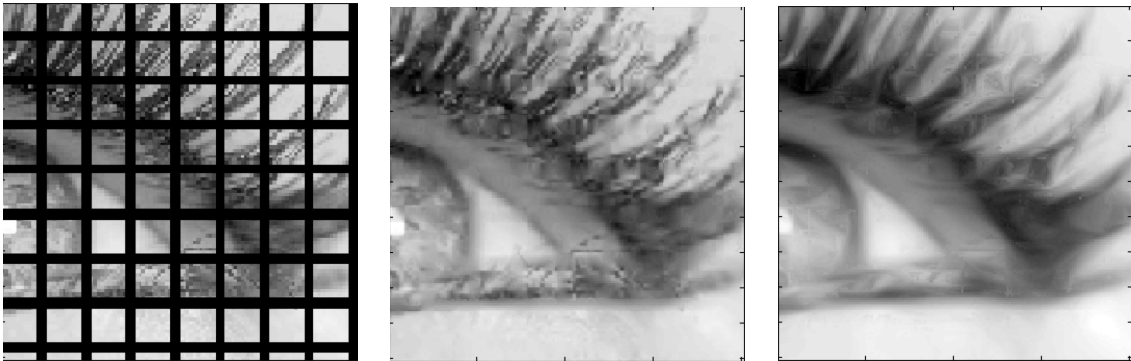


Figure 13. From left to right: a detail of the original image (courtesy of Boscain et al. [9]); a detail of the image inpainted using the proposed algorithm; the same detail of the image inpainted and enhanced with this algorithm.

Definition A.2 (horizontal divergence). The horizontal divergence of a horizontal vector $w = w_1X_1^0 + w_2X_2^0$ is defined as follows:

$$\operatorname{div}_0(w) = X_1^0(w_1) + X_2^0(w_2).$$

Definition A.3 (Laplace–Beltrami operator). The Laplace–Beltrami is a second order operator on the horizontal tangent space to the surface (i.e., the subset of the horizontal bundle which is tangent to the manifold). In the present setting we consider the surface

$$S = \{(x, y, \theta) : u(x, y, \theta) = 0\},$$

which has a unique tangent vector field (see (4)):

$$T_0 = \frac{X_2^0 u X_1^0 - X_1^0 u X_2^0}{|\nabla_0 u|}.$$

If $v : S \rightarrow \mathbb{R}$ we will call the Laplace–Beltrami operator the second derivative in the direction of the vector T_0 :

$$\Delta_{LB} v = T_0^2 v.$$

Finally we recall that the notion of increment on a manifold is replaced by the notion of exponential map.

Definition A.4 (exponential map). *Let v be a vector field tangent to a differentiable manifold M , and let $p \in M$. Then there is a unique solution of the Cauchy problem $\gamma' = v$ with initial condition $\gamma_v(0) = p$. If the norm of v is sufficiently small, the solution can be extended up to the time $t = 1$ and the exponential map is defined*

$$\exp_p(v) = \gamma_v(1).$$

REFERENCES

- [1] G. BARLES AND P.E. SOUGANIDIS, *Convergence of approximation schemes for fully nonlinear second order equations*, *Asymptot. Anal.*, 4 (1991), pp. 271–283.
- [2] J. BENCE, B. MERRIMAN, AND S. OSHER, *Diffusion generated motion by mean curvature*, in *Computational Crystal Growers Workshop*, J. Taylor, ed., AMS, Providence, RI, 1992.
- [3] M. BERTALMIO, G. SAPIRO, V. CASELLES, AND C. BALLESTER, *Image Inpainting*, in *Proceedings of SIGGRAPH 2000*, New Orleans, LA, 2000.
- [4] M. BERTALMIO, V. CASELLES, S. MASNOU, AND G. SAPIRO, *Inpainting*, in *Encyclopedia of Computer Vision*, Springer, New York, 2011.
- [5] T. BIESKE, *On ∞ -harmonic functions on the Heisenberg group*, *Comm. Partial Differential Equations*, 27, (2002), pp. 727–761.
- [6] T. BIESKE, *Comparison principle for parabolic equations in the Heisenberg group*, *Electron. J. Differential Equations* (2005), 95.
- [7] W. BOSKING, Y. ZHANG, B. SCHOFIELD, AND D. FITZPATRICK, *Orientation selectivity and the arrangement of horizontal connections in tree shrew striate cortex*, *J. Neurosci.*, 17 (1997), pp. 2112–2117.
- [8] U. BOSCAIN, J. DUPLAIX, J.P. GAUTHIER, AND F. ROSSI, *Anthropomorphic image reconstruction via hypoelliptic diffusion*, *SIAM J. Control Optim.*, 50 (2012), pp. 1309–1336.
- [9] U. BOSCAIN, R.A. CHERTOVSKIH, J.P. GAUTHIER, AND A.O. REMIZOV, *Hypoelliptic diffusion and human vision: A semidiscrete new twist*, *SIAM J. Imaging Sci.*, 7 (2014), pp. 669–695.
- [10] L. CAPOGNA AND G. CITTI, *Generalized mean curvature flow in Carnot groups*, *Comm. Partial Differential Equations*, 34 (2009).
- [11] L. CAPOGNA, G. CITTI, AND M. MANFREDINI, *Regularity of Mean Curvature Flow of Graphs on Lie Groups Free up to Step 2*, arXiv:1502.00874, 2015.
- [12] L. CAPOGNA, G. CITTI, AND M. MANFREDINI, *Regularity of non-characteristic minimal graphs in the Heisenberg group H^1* , *Indiana Univ. Math. J.*, 58 (2009), pp. 2115–2160.
- [13] L. CAPOGNA, D. DANIELLI, S. PAULS, AND J. TYSON, *An Introduction to the Heisenberg Group and the Subriemannian Isoperimetric Problem*, *Progr. Math.*, 259, Birkhäuser-Verlag, Basel, 2007.
- [14] Y.-G. CHENG, Y. GIGA, T. HITAKA, AND M. HONMA, *Numerical Analysis for Motion of a Surface by Its Mean Curvature*, Hokkaido University, 1993.
- [15] J.-H. CHENG, J.-F. HWANG, A. MALCHIODI, AND P. YANG, *Minimal surfaces in pseudohermitian geometry*, *Ann. Sc. Norm. Super. Pisa Cl. Sci.*, (5) 4, no. 1, pp. 129–177, (2005).
- [16] J.-H. CHENG, J.-F. HWANG, AND P. YANG, *Regularity of C^1 smooth surfaces with prescribed p -mean curvature in the Heisenberg group*, *Math. Ann.*, 344 (2009), pp. 1–35.
- [17] Y. CHEN, Y. GIGA, AND S. GOTO, *Uniqueness and existence of viscosity solutions of generalized mean curvature flow equations*, *J. Differential Geom.*, 33 (1991), pp. 749–786.
- [18] G. CITTI AND A. SARTI, *A cortical based model of perceptual completion in the roto-translation space*, *J. Math. Imaging Vision*, 24 (2006), pp. 307–326.
- [19] G.-H. COTTET AND L. GERMAIN, *Image processing through reaction combined with nonlinear diffusion*, *Math. Comp.*, 61 (1993), pp. 659–667.
- [20] M.G. CRANDALL, H. ISHII, AND P.-L. LIONS, *User’s guide to viscosity solutions of second order partial differential equations*, *Bull. Amer. Math. Soc. (N.S.)*, 27 (1992), pp. 1–67.

- [21] M.G. CRANDALL AND P.L. LIONS, *Convergent Difference Schemes for Nonlinear Parabolic Equations and Mean Curvature Motion*, Springer-Verlag, Berlin, 1996.
- [22] D. DANIELLI, N. GAROFALO, AND D.M. NHIEU, *Sub-Riemannian calculus on hypersurface in Carnot groups*, *Adv. Math.*, 215 (2006), pp. 292–378.
- [23] K. DECKELNICK, *Error bounds for a difference scheme approximating viscosity solutions of mean curvature flow*, *Interfaces Free Bound.*, 2 (2000), pp. 117–142.
- [24] K. DECKELNICK AND G. DZIUK, *Convergence of Numerical Schemes for the Approximation of Level Set Solutions to Mean Curvature Flow*, World Scientific, River Edge, NJ, 2001.
- [25] N. DIRR, F. DRAGONI, AND M. VON RENESSE, *Evolution by mean curvature flow in sub-Riemannian geometries: A stochastic approach*, *Commun. Pure Appl. Anal.*, 9 (2010), pp. 307–326.
- [26] R. DUITTS, M. DUITTS, M. VAN ALMSICK, AND B.M. TER HAAR ROMENY, *Invertible orientation scores as an application of generalized wavelet theory*, *Pattern Recognition Image Anal.*, 17 (2007), pp. 42–75.
- [27] R. DUITTS AND E.M. FRANKEN, *Left-invariant parabolic evolution equations on $SE(2)$ and contour enhancement via invertible orientation scores, Part I: Linear left-invariant diffusion equations on $SE(2)$* , *Quart. Appl. Math.*, 68 (2010), pp. 255–292.
- [28] R. DUITTS AND E.M. FRANKEN, *Left-invariant parabolic evolution equations on $SE(2)$ and contour enhancement via invertible orientation scores, Part II: Nonlinear left-invariant diffusion equations on invertible orientation scores*, *Quart. Appl. Math.*, 68 (2010), pp. 293–331.
- [29] L.C. EVANS AND J. SPRUCK, *Motion of level sets by mean curvature*, in *Int. J. Diff. Geom.*, 33 (1991), pp. 635–681.
- [30] F. FERRARI, Q. LIU, AND J.J. MANFREDI, *On the horizontal mean curvature flow for axisymmetric surfaces in the Heisenberg group*, *Discrete Contin. Dyn. Syst.*, 34 (2013), pp. 2779–2793.
- [31] D. FIELD, A. HEYES, AND R.F. HESS, *Contour integration by the human visual system: Evidence for a local association field*, *Vision Research*, 33 (1993), pp. 173–193.
- [32] B. FRANCHI, R. SERAPIONI, AND F. SERRA CASSANO, *Regular hypersurfaces, Intrinsic perimeter and implicit function theorem in Carnot groups*, *Comm. Anal. Geom.*, 11 (2002), pp. 909–944.
- [33] E.M. FRANKEN AND R. DUITTS, *Crossing-preserving coherence-enhancing diffusion on invertible orientation scores*, *Int. J. Comput. Vis.*, 85 (2009), pp. 253–278.
- [34] M. GALLI AND M. RITORÉ, *Regularity of C^1 surfaces with prescribed mean curvature in 3-dimensional contact sub-Riemannian manifolds*, *Calc. Var. Partial Differential Equations*, 54 (2015), pp. 2503–2516.
- [35] M. GROMOV, *Carnot-Carathéodory spaces seen from within*, in *Sub-Riemannian Geometry*, *Progr. Math.* 144, Birkhauser, Basel, 1996.
- [36] R.K. HLADKY, *Connections and curvature in a sub-Riemannian geometry*, *Houston J. Math.*, 38 (2012), pp. 1107–1134.
- [37] R.K. HLADKY AND S.D. PAULS, *Constant mean curvature surfaces in sub-Riemannian geometry*, *J. Differential Geom.*, 79 (2008), pp. 111–139.
- [38] W.C. HOFFMAN, *The visual cortex is a contact bundle*, *Appl. Math. Comput.*, 32 (1989), pp. 137–167.
- [39] L. HÖRMANDER, *Linear Partial Differential Operators*, Springer-Verlag, Berlin, 1963.
- [40] L. HÖRMANDER, *Hypoelliptic second order differential equations*, *Acta Math.*, 119 (1967), pp. 147–171.
- [41] B. HORN, *The curve of least energy*, *ACM Trans. Math. Software*, 9 (1983), pp. 441–460.
- [42] D. HUBEL AND T. WIESEL, *Receptive fields, binocular interaction and functional architecture in the cat's visual cortex*, *J. Physiology*, 160 (1962), pp. 106–154.
- [43] D. HUBEL AND T. WIESEL, *Ferrier lecture: Functional architecture of macaque monkey visual cortex*, *Proc. R. Soc. Lond. Ser. B*, 198 (1977), pp. 1–59.
- [44] H. ISHII, *Viscosity solutions of nonlinear partial differential equations in Hilbert spaces*, *Comm. Partial Differential Equations*, 18 (1993).
- [45] D. JERISON, *The Poincaré inequality for vector fields satisfying the Hörmander's condition*, *Duke Math. J.* 53 (1986), pp. 503–523.
- [46] G. KANIZSA, *Grammatica del vedere*, Il Mulino, Bologna, 1980.
- [47] R. KIMMEL, R. MALLADI, AND N. SOCHEN, *Images as Embedded Maps and Minimal Surfaces: Movies, Color, Texture and Volumetric Medical Images*, *Int. J. Comput. Vision*, 39 (2000), pp. 111–129.
- [48] J.J. KOENDERINK AND A.J. VAN DOORN, *Representation of local geometry in the visual system*, *Biol. Cybernet.*, 55 (1987), pp. 367–375.

- [49] O.A. LADYZENSKAJA, V.A. SOLONNIKOW, AND N.N. URAL'CEVA, *Linear and Quasilinear Equations of Parabolic Type*, Transl. Math. Monogr. 23, AMS, Providence, RI, 1967.
- [50] S. MASNOU AND J.M. MOREL, *Level-lines based disocclusion*, in Proceedings of the 5th IEEE International Conference on Image Processing, Chicago, IL, 1998.
- [51] B. MERRIMAN, J. BENCE, AND S. OSHER, *Diffusion Generated Motion by Mean Curvature*, CAM Report 02-18, UCLA, 1992.
- [52] D. MUMFORD, *Elastica and computer vision*, in Algebraic Geometry and Its Applications, Springer, New York, 1994, pp. 491–506.
- [53] A. NAGEL, E.M. STEIN, AND S. WAINGER, *Balls and metrics defined by vector fields: Basic properties*, Acta Math. (1985).
- [54] M. NITZBERG, D. MUMFORD, AND T. SHIOTA, *Filtering, Segmentation, and Depth*, Springer-Verlag, Berlin, 1993.
- [55] M. NITZBERG AND T. SHIOTA, *Nonlinear image filtering with edge and corner enhancement*, IEEE Trans. Pattern Anal. Machine Intelligence, 14 (1992), pp. 826–833.
- [56] S. OSHER AND J.A. SETHIAN, *Fronts propagating with curvature dependent speed: Algorithms based on Hamilton-Jacobi formulations*, J. Comput. Phys., 79 (1988), pp. 12–49.
- [57] S.D. PAULS, *H-minimal graphs of low regularity in H^1* , Comment. Math. Helv., 81 (2006), pp. 337–381.
- [58] J. PETITOT, *The neurogeometry of pinwheels as a sub-Riemannian contact structure*, J. Physiol. Paris, 97 (2003), pp. 265–309.
- [59] J. PETITOT AND Y. TONDUT, *Vers une Neuro-geometrie, Fibrations corticales, structures de contact et contours subjectifs modaux*, Math. Inf. Sci. Hum. 145 (1998), pp. 5–101.
- [60] D. PRANDI, A. REMIZOV, R. CHERTOVSKIH, U. BOSCAIN, AND J.P. GAUTHIER, *Highly Corrupted Image inpainting Through Hypoelliptic Diffusion*, arXiv:1502.07331, 2015.
- [61] M. RITORÉ AND M.C. ROSALES, *Area stationary surfaces in the Heisenberg group H^1* , Adv. Math., 219 (2008), pp. 633–671.
- [62] L.P. ROTHSCHILD AND E.M. STEIN, *Hypoelliptic differential operators and nilpotent groups*, Acta Math., 137 (1976), pp. 247–320.
- [63] G. SANGUINETTI, *Invariant Models of Vision Between Phenomenology, Image Statistics and Neurosciences*, Universidad de la Republica, Montevideo, 2011.
- [64] G. SANGUINETTI, G. CITTI, AND A. SARTI, *Implementation of a model for perceptual completion in $\mathbb{R}^2 \times S^1$* , Computer Vision and Computer Graphics. Theory and Applications, Springer, Berlin, 2009.
- [65] A. SARTI AND G. CITTI, *A cortical based model of perceptual completion in the roto-translation space*, in Proceeding of the Workshop on Second Order Subelliptic Equations and Applications, Cortona, 2003.
- [66] A. SARTI, G. CITTI, AND J. PETITOT, *The symplectic structure of the visual cortex*, Biol. Cybernet, 98 (2008), pp. 33–48.
- [67] A. SARTI, R. MALLADI, AND J.A. SETHIAN, *Subjective surfaces: A geometric model for boundary completion*, Internat. J. Comput. Vision, 46 (2002), pp. 201–221.
- [68] D. TSCHUMPER, *Fast anisotropic smoothing of multi-valued images using curvature-preserving PDEs*, Internat. J. Comput. Vision, 68 (2006), 65.
- [69] S. ULLMAN, *Filling-in the gaps: The shape of subjective contours and a model for their generation*, in Biological Cybernetics, Springer-Verlag, Berlin, 1976.
- [70] C.Y. WANG, *The Aronsson equation for absolute minimizers of L^∞ functionals associated with vector fields satisfying Hörmanders condition*, Trans. Amer. Math. Soc., 359 (2007), pp. 91–113.
- [71] C.Y. WANG, *Viscosity convex functions on Carnot groups*, Proc. AMS, 133 (2005), pp. 1247–1253.
- [72] J.A. WEICKERT, *Anisotropic Diffusion in Image Processing*, Eur. Consort. Math. Ind., Teubner, Stuttgart, 1998.
- [73] J.A. WEICKERT, *Coherence-enhancing diffusion filtering*, Internat. J. Comput. Vis., 31 (1999), pp. 111–127.
- [74] S.W. ZUCKER, *The curve indicator random field: Curve organization via edge correlation*, in Perceptual Organization for Artificial Vision Systems, Kluwer Academic, Dordrecht, 2000, pp. 265–288.